An Experimental Investigation of Slip-Stick Friction in a Block-Spring Earthquake Model

Ben Stern
Department of Physics, The College of Wooster, Wooster, OH 44691, USA
(Dated: May 3, 2021)

A block-spring earthquake model was investigated experimentally for a one-block system, and the behavior was characterized according to the rate- and state- dependent friction theory developed by Dieterich and Ruina. Position data was recorded for the block as it was driven by a constant velocity driver, and the behavior was characterized as stick-slip, non-stick-slip self-sustained oscillations, or stable sliding. Slip-stick and oscillatory behavior indicated velocity-weakening systems, while stable sliding indicated velocity-strengthening systems. The systems were characterized by the type of materials in contact during the sliding: PVC and aluminum, nitrile, or cardstock. Cardstock exhibited the most stick-slip behavior while aluminum lead to distinctly velocity-strengthening behavior. Nitrile trials were largely inconclusive. Furthermore, increasing the spring strength stabilized the system for the cardstock, which further validates the theory for velocity-weakening friction .

I. INTRODUCTION

Of all the pseudo-forces in physics, friction is certainly one of the most ubiquitous. Truly, we live in a world governed by friction. One imagines a world in which friction did not exist – an ice-rink of the eternally adrift – and is quickly thankful to have one's feet planted firmly on the ground. Possibly only the introductory physics student might find reason to object...and this student would have good reason. After all, friction is notoriously difficult to model!

In fact, definitive friction models remain elusive. As a non-conservative force, friction is difficult to describe purely theoretically due to the inherent energy loss. However, friction's ubiquity is an advantage in the experimental realm, where the available systems governed by friction are plentiful. Thus, there has been success in developing empirical friction models, particularly in the latter 20th century up to present day. This progress is of particular importance given the impact of friction on our daily lives, both favorable and adverse. We can thank friction for the traction of our car tires on the road, but also the occurrence of earthquakes which can wreak devastation. Thus, there is real significance to the creation of these friction models, with interdisciplinary applications.

Earthquakes are a particularly famous example of complex frictional motion, where tectonic plates in the Earth's crust slide against each other and their motion is controlled by dynamic friction. This motion can be modeled using a simple array of blocks connected by springs, famously discovered by Burridge and Knopoff in the 1960s [1]. This Burridge-Knopoff model was then improved by Dieterich [2] and Ruina [3] in the 1970s and 1980s to create the rate- and state- dependent friction equations which are still currently in wide use given how effective they are at describing the complex, and often chaotic, behavior of earthquakes [4]. Earthquakes are notoriously difficult to predict, and so harnessing these equations to effectively model their motion would be an incredibly powerful tool. Papers by Erickson [4], Kostic [5], Chen [6], and others continue to develop this theory and explore the complex nonlinear dynamics of earthquake motion, mainly through computational simulation.

This paper will explore the rate- and state- dependent friction equations and work to verify the implications of the theory experimentally for a one-block system.

II. THEORY

When cracks propagate through the Earth's crust, faults are formed and the subsequent motion of these interacting rock segments is controlled by friction. The rocks stick together along the fault line, held together by static friction, until they suddenly slip, resulting in an earthquake. This stick and slip behavior is complex and modeling requires more sophisticated methods than the well-known static and dynamic friction theories – particularly, the rate- and state- dependent friction model. First, however, it is necessary to characterize friction at the microscopic level.

A. Asperities and Real Contact

The macroscopic effects of friction are well known and easily observed; rub one's hands together and there is a clear resistance to the motion due to friction at the plane of contact. So, what is truly going on at the microscopic level?

If one were to zoom in on the contact between two materials, perhaps a fault between two rocks, it might look like Fig. 1a, where the *true* contact occurs between the irregular bumps and protrusions along the surfaces, called asperities. When these surfaces slide against each other, the asperities may interlock and exert a force opposing this sliding motion. This is friction in action, at a microscopic level.

It follows, then, that the magnitude of the friction force correlates to the number of asperity contacts. Furthermore, one can add up all of these points of contact to

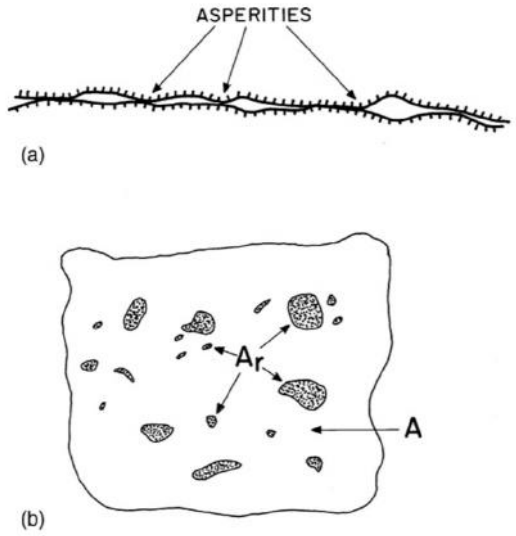

FIG. 1: Schematic of contact between two materials. Part (a) depicts a close-up view of contact between two materials, where real contact occurs at the asperities. Part (b) shows the macroscopic view of real contact area, where each darkened region is composed of tiny asperity contacts. Necessarily, real contact A_r is smaller than surface area A. Figure from [7].

get the area of real contact A_r – a distinct quantity from the more traditional surface area A. Real contact area is visualized in Fig. 1b where the darkened patches indicate areas of real contact, composed of lots of tiny asperities, and $Ar < A$. The natural conclusion then, is that friction is determined by the real contact area A_r, *independent of the total surface area.* Indeed, this concept agrees with the well-known formulation for friction,

$$F_\mu = N\mu, \tag{1}$$

where N is the normal force pushing on the surface and μ is the coefficient of friction. If N is equal to the weight on an object, say for a book sitting on a flat tabletop, then adding masses on top of the book will increase the weight, and thus increasing N and F_μ. Conceptually, increasing the weight of the book would increase the real contact area between the book and the table, as additional asperity contacts are created through the materials being pressed closer together, and thus the friction force would increase, as predicted by Eq. 1. This relationship between friction and normal forces, as determined by the real contact area, is critical for describing more complicated friction such as stick-slip.

B. Stick-Slip Motion

Consider a block pulled by a spring across a rough surface, as in Fig. 2a, where the spring is pulled by a constant velocity driver. There are two forces affecting motion in the x-direction: a pulling force by the spring, F_s,

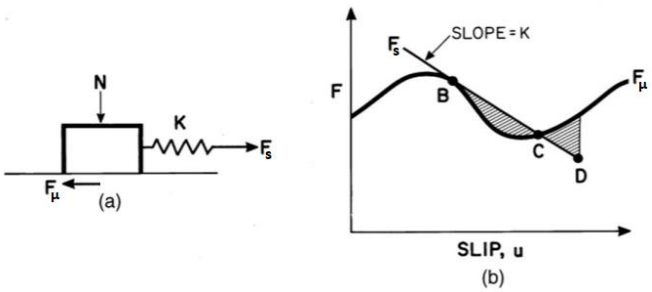

FIG. 2: (a) A block is pulled by a spring of stiffness k across a rough surface, where friction F_μ is determined by the normal force N. (b) A diagram of the friction and spring forces acting on the block. The block slips at B, the point of instability, and speeds up until C where it starts to slow down until it sticks again at D. Figure adapted from [7].

and a damping force due to friction, F_μ. As in any Newtonian mechanics problem, the balance of these forces determines if the block is speeding up, slowing down, or moving at a constant speed.

Experiment has shown that friction is not a constant force, but a dynamic one. Thus, we see in Fig. 2b a dynamic friction force F_μ for our block (a) juxtaposed with the linear spring force $F_s = -ku$. The spring begins maximally engaged before point B, and then decompresses as the block slips. Point B indicates the threshold for instability, where F_μ decreases faster than F_s and so the block speeds up due to the force imbalance, otherwise known as a slip. At point C, F_μ overtakes F_s and the block slows down until it sticks at point D. The area of the shaded regions are equal, as the net work required to speed the block up from B to C must equal the net work to slow the block down the same amount from C to D. If B is the point that initiates instability, it follows then that the condition for instability is,

$$\left|\frac{\partial F}{\partial u}\right| > k, \tag{2}$$

and this unstable region implies stick-slip motion [7].

However, the question remains, what would cause a system to behave according to Fig. 2 and Eq. 2? The answer is simply that F_μ must decreases for higher slip velocities, indicating a *velocity-weakening system.* Ruina [3] first demonstrated how a velocity-strengthening system will never lead to regular stick-slip motion as the increase in friction with slip velocity damps the system so that condition Eq. 2 is not met, and no instability occurs. Thus, velocity-weakening is a necessary condition for regular stick slip motion to occur, whereas velocity strengthening *always* results in stable sliding. [7]

C. Rate- and State-Dependent Friction

Through the mid 20th century there were efforts to create mathematical velocity-weakening models for stick-slip friction, but none were ultimately successful until Dieterich [2] and Ruina [3] developed the rate- and state-friction laws (RSF) in the 1970s and 1980s. The key improvement they made to previous models was the inclusion of a state variable θ to describe the contact between the surfaces, and how this contact evolves through time [7]. The precise physical interpretation of θ remains unknown, where it may possibly be characterized by temperature, pore pressure, the chemical environment, or the average asperity contacts between the surfaces [2, 4].

Not only is θ itself an unknown quantity, the way that it evolves remain an open problem. The most common state evolution equations were proposed by Dieterich and Ruina – the Aging Law and the Slip Law respectively. Dieterich's law takes the form

$$\dot{\theta} = 1 - \frac{V\theta}{D_c}, \tag{3}$$

where $\theta = t$ when $V = 0$; in other words, when the block is stationary the state still increases with time, which agrees with experiment [7]. Conversely, Ruina's law

$$\dot{\theta} = -\frac{V\theta}{D_c} \tag{4}$$

does not allow for state evolution when $V = 0$, but it has proven to agree with experiment during a slip event. In both Eqs. 3 and 4, D_c indicates the critical slip distance required for the system to reach steady-state, $\dot{\theta} = 0$, and is usually on the order of micrometers [7]. Thus, at the steady-state, $D_c = V_{ss}\theta_{ss}$ where V_{ss} is the steady-state slip velocity and θ_{ss} is the steady state [7].

Now that we have characterized the state variable θ, we can use it to describe stick-slip friction. Specifically, since the normal force N is constant, μ must be the dynamic element of Eq. 1, and can be written as a function of slip velocity V and state θ,

$$\mu \equiv \mu(V, \theta) = \mu_0 + b \ln\left(\frac{V_0\theta}{L}\right) + a \ln\left(\frac{V}{V_0}\right). \tag{5}$$

This equation was, again, developed by Dieterich and Ruina, and depends on a constant driving velocity V_0, and constants a and b. These a and b parameters are particularly important in characterizing a system as velocity weakening, and they are best understood through consideration of Fig. 3.

Reading Fig. 3 from left to right, the block has an initial velocity V_0 with constant friction until it undergoes a sharp velocity jump to a new velocity V, at which point the friction also spikes by a. As the block slips the friction decays exponentially by b, approaching the value $(a - b)$. This velocity-stepping process can then be repeated for a negative change in velocity and the plot inverts. The

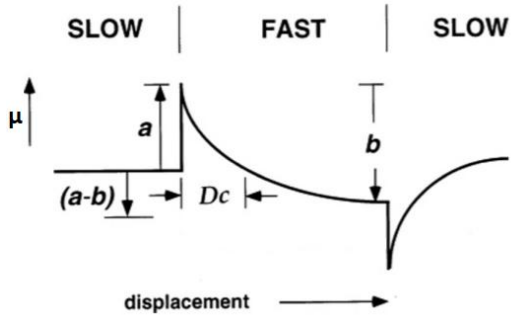

FIG. 3: A velocity weakening system. A sudden velocity increase occurs where μ spikes up a distance a, where $V_0 \to V$ for $V = eV_0$ necessarily to define a. D_c characterizes the slip distance to achieve the steady state θ_{ss}. a characterizes the initial increase in frictional stress due to increase in slip velocity, and b characterizes the exponential decay until the block sticks. For a sudden e-fold decrease in velocity the behavior is inverted. Figure adapted from [7].

variable D_c indicates the distance required for the block to achieve the steady-state.

Importantly, a is defined by an e-fold change in velocity where $V = eV_0$, so that when plugged into Eq. 5 we get

$$\Delta\mu = a \ln\left(\frac{V}{V_0}\right) = a \ . \tag{6}$$

We can also define the total change in friction $(a - b)$ by considering the steady-state friction μ_{ss}. Recall that for the steady state, $V_{ss}\theta_{ss} = D_c$, and so Eq. 5 becomes

$$\mu_{ss} = \mu_0 + (a - b) \ln\left(\frac{V_{ss}}{V_0}\right). \tag{7}$$

If we then differentiate Eq. 7 with respect to $\ln V_{ss}$, we get a definition for $(a - b)$,

$$\frac{d\mu_{ss}}{d(\ln V_{ss})} = (a - b). \tag{8}$$

Thus, assuming that D_c is small so the block is in the steady-state for the entirety of the slip, $(a-b)$ characterizes the change in μ over the course of a slip. This quality is apparent from Fig. 3. Furthermore, from Fig. 3 we see that $(a - b) < 0$ characterizes the system as velocity-weakening, given the net decrease in friction due to an increase in velocity. In the context of asperity contacts, the "viscous" term a determines the shearing rate of real contacts at the onset of a slip which results in a sudden increase in friction, and the "healing" term b characterizes the rate of change of real contact area due to a sudden velocity change. To that end, a is related to the shearing deformation of the material and b is related to normal deformations. The interplay of $(a - b)$ determines if the system is velocity weakening, and thus if the system will exhibit stick slip motion. [7]

D. Instability in a Velocity-Weakening System

A velocity-weakening system always has the ability to exhibit stick-slip motion, but the system must meet a condition of instability in order to do so. Particularly, there is a critical value of normal stress σ_n that determines the stability of the system. As one might expect, σ_c depends on $(a-b)$,

$$\sigma_c = \frac{kD_c}{(a-b)}, \tag{9}$$

where values of $\sigma_n > \sigma_c$ indicate instability and thus stick-slip motion. Noticeably, this critical stress is proportional to the spring constant k, along with the other constants that define the sliding material. Fig. 4 plots the necessary velocity change ΔV for a system to undergo unstable slip, below which the system will settle to stable sliding. Thus, σ_c is a bifurcation point for the system's behavior, where values of $\sigma_n < \sigma_c$ indicate conditional stability and will only experience stick-slip motion for sufficiently high ΔV. Near the critical stress, but still less than σ_c, the motion becomes oscillatory but not quite stick-slip.

Geologically, Fig. 4 provides an important overview of the necessary conditions for earthquake motion. Earthquakes will only nucleate in the stick-slip region where $\sigma_n > \sigma_c$. The region of self-sustained oscillations corresponds to periodic slow-slip events.

III. PROCEDURE

A. Experimental Design

Stick-slip friction was investigated using an aluminum block of mass 235 g, pulled across a sliding platform by a low-friction PASCO cart, attached with a spring. Fig. 5a shows an image of this setup, including the PASCO Motion Sensor II used to record the position of the block. Fig. 5b depicts a schematic of this configuration where the cart moves at velocity V_0, the block slips with velocity V, and the spring has stiffness k. The sliding platform, seen best in Fig. 6, was a 91.5 cm long metal sheet covered in a 1 mm thick vinyl (PVC) mat. The cart is pulled via a 970 rpm gear motor and pulley, driven by a TP3005DM DC power supply.

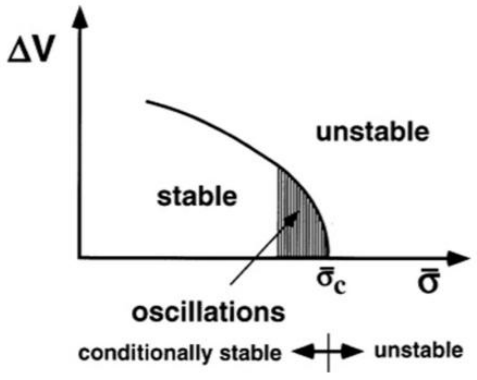

FIG. 4: Plot indicates the stability for a velocity weakening system, as a function of the effective normal stress σ_n. Below the critical value σ_c, a given velocity perturbation ΔV must exceed the curve for instability to occur. Near the critical point the system will exhibit self-sustained oscillations. Figure from [7]

TABLE I: Springs and their measured k values.

Spring	k (N/m)
A	4.83 ± 0.02
B	9.61 ± 0.09
C	20.2 ± 0.2

B. Data Collection

1. Calibration

The spring constants of three springs were measured by hanging masses from each spring and recording the displacement. Mass and displacement were plotted according to Hooke's law, $mg = kx$, where k was the slope. Values of k for each spring, A, B, C, and D, can be found in Table. I.

The driving velocity was calculated for voltage 2.6 V, through an average of three trials. For each trial the cart was pulled across the platform and position data was recorded. Velocity was determined from the slope of each position plot and averaged to $V_0 = 0.205$ m/s with a standard deviation of 0.004 m/s.

2. Stick-Slip Trials

The system's behavior was explored for different sliding contact surfaces and for different spring strengths. Each trial used the PVC platform, but different materials were attached to the block's bottom face, yielding distinct types of contact with the PVC. Specifically, three materials were used: aluminum (the block itself), nitrile rubber, and cardstock. For each surface, springs A, B, and C were used, with measured strengths found in Table I.

A given trial was conducted by pre-setting the power supply to 2.6 V so that the power could be switched on to the correct voltage immediately, providing clean data for the entirety of the slip. The positions of the block and cart were both recorded by motion sensors, one at each end of the sliding platform.

A constant voltage 2.6 V was used for all trials, in order to isolate the sliding material and spring strength as experimental parameters. When calibrated, this voltage

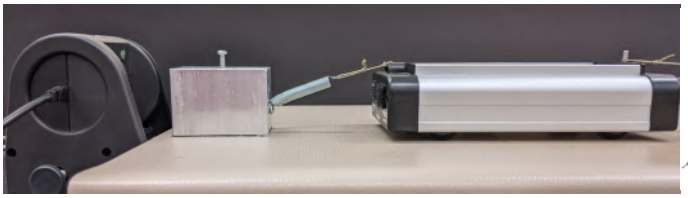

(a)

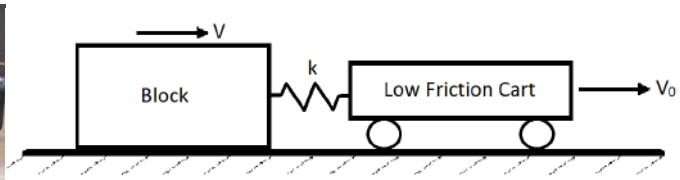

(b)

FIG. 5: A spring block system pulled by a constant velocity driver. (a) is the experimental setup, with an aluminum block pulled by a low-friction cart with a spring, across a textured 1 mm vinyl surface. A Pasco motion sensor tracks the position of the block. (b) depicts a schematic of the setup, where the cart moves at constant V_0 and pulls the block with spring k, and the block slips with velocity v.

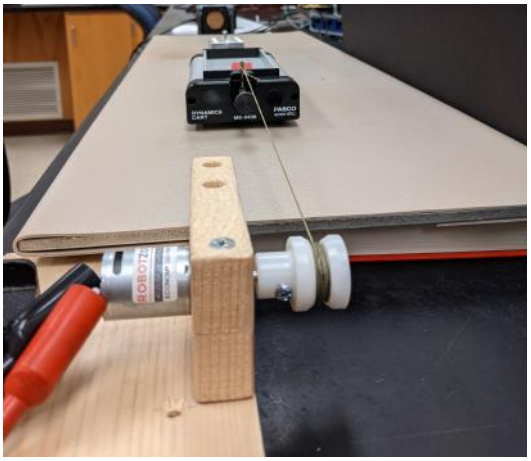

FIG. 6: A power supply drives the motor-pulley system which is clamped firmly to the lab bench, and pulls the cart-spring-block system across the PVC sliding platform while the motion sensor records position data.

corresponded to a speed $V_0 = 0.205 \pm 0.004$ m/s; however, when a block was attached to the cart, the average driving velocity decreased noticeably below one standard deviation. For example, when using cardstock the average driving voltage decreased by 0.058 m/s for spring C, 0.69 m/s for spring B, and 0.083 m/s for spring A. Thus, the average driving voltage for each trial decreases as the spring strength decreases.

IV. RESULTS & ANALYSIS

A. Qualitative Material Properties

Before analyzing the block-spring data, it is pertinent to consider the qualities of the materials used, in the context of the theory of velocity-weakening and velocity-strengthening systems. This discussion will be somewhat speculative in regard to the microscopic qualities of these materials, given the limitations of laboratory equipment and time to conduct a thorough empirical investigation of material properties. Future work would certainly involve measuring the viscous term a, healing term b, and characteristic length D_c for these materials. Despite the current limitations for measuring these constants, given how important they are in controlling the sliding motion of the block they are worth discussing qualitatively.

The sliding surface material is the same for each trial, PVC, and so its inherent properties are certainly an important factor in the block's motion, as well as the asperity interactions between PVC and each of the other materials – aluminum, nitrile, and cardstock. The 1 mm thick PVC mat is somewhat cushioned and elastic so that it compresses under pressure and returns to its original configuration. It is also textured to the touch, rather than slick. These distinct qualities suggest that the PVC likely maximizes its real contact area more than the other materials. The inherent elasticity could imply that asperity contacts would be restored readily throughout a slip event, which would correlate to a smaller b value, according to Fig. 3. If real contact area increases quickly, friction would be restored quickly and the velocity-weakening effects would be mitigated. However, this does not necessarily imply that $a < b$; likely, the value of a would depend on the nature of the contact of the PVC with the other material.

Aluminum is a soft metal, but still more rigid than the other materials used in this experiment. Rigid asperities in the metal's surface could result in a greater induced frictional stress at the onset of a slip as static friction is overcome, and thus would imply a larger value of a by Fig 3. Furthermore, the aluminum was observed to adhere slightly to the PVC, as though through a slightly "sticky" contact, which would also contribute to this increased frictional stress at the onset of slip. Given these observations, one can hypothesize that PVC-metal is a velocity strengthening system with $(a - b) > 0$. Indeed, this is found to be true through data analysis.

Cardstock is the next most rigid material, next to aluminum, but the asperities in the paper surface likely shear more easily than aluminum. However, cardstock also adhered somewhat to the "sticky" PVC surface. These observations could imply a value of a smaller than for aluminum, however to this author they do nothing to suggest the size of a in comparison to b.

Nitrile's rigidity likely falls somewhere between the

PVC and cardstock, and has a similar sticky quality as the PVC. Nitrile, however, is more elastic than PVC. The combination of both nitrile and PVC's malleability likely results in the largest real contact area of all the material combinations, and their elastic properties would imply relatively quick frictional healing. Thus, one might expect the nitrile-PVC contact to have a large b value. The value of a, however, is somewhat more difficult to predict qualitatively.

B. Slip-Stick

Block position data is displayed in Fig. 7 with distinct plots for each combination of materials – PVC with either aluminum, nitrile, or cardstock. The spring strengths are indicated by color in each plot, for springs A, B, and C. With nine combinations of sliding materials and springs, a variety of behaviors are found in this data, many of which correspond well to the theory.

First, some general trends. Across all plots (a), (b), and (c), the time before the initial slip increased with decreasing spring strength, so spring A took the longest time to slip and spring C took the shortest time. This makes sense, given that spring A is the weakest and spring C the strongest. In fact, spring A was weak enough that for plots (a) and (b) the block remained stuck so long that the cart had nearly reached the end of the platform by the time the first slip occurred. Thus, there is not much analyzable motion for the plots (a) and (b) for spring A.

The sliding material appeared to have the greatest impact on the stability of the system, where cardstock exhibited slip-stick motion the most readily of the three materials. No slip-stick behavior was found for nitrile but there were oscillations, and aluminum exhibited only brief stick-slip behavior for spring B. All slip-stick and oscillatory behavior was periodic, as demonstrated in Fig. 8 for the trials of cardstock with spring B (slip-stick) and nitrile with spring C (tremors). For each of these position traces, the time of a given slip was found by fitting the curve with a straight line and then plotting the residual. The maximum negative deviations from the linear fit indicated the beginning of a slip, or equivalently the end of a stick, and these times were plotted in Figs. 8b and 8d.

These systems can be examined in the context of Fig. 4 to characterize their level of stability or instability. Recall from Eq. 9 that $\sigma_c \propto k$, so for a given material defined by constants a, b, and D_c, a higher spring strength corresponds to a higher critical stress; thus, by Fig. 4, for certain k the system will have normal stress near σ_c and undergo self-oscillatory slips within a range of initial slip velocities ΔV beneath the curve in Fig. 4.

Fig. 7c suggests that cardstock results in regular stick-slip, and thus cardstock is a good candidate for a velocity-weakening system. Of course, this cannot be asserted with absolute certainty as velocity-weakening is defined by longterm behavior and the sliding distance can only be 80 cm at most, so the experimental design does not allow

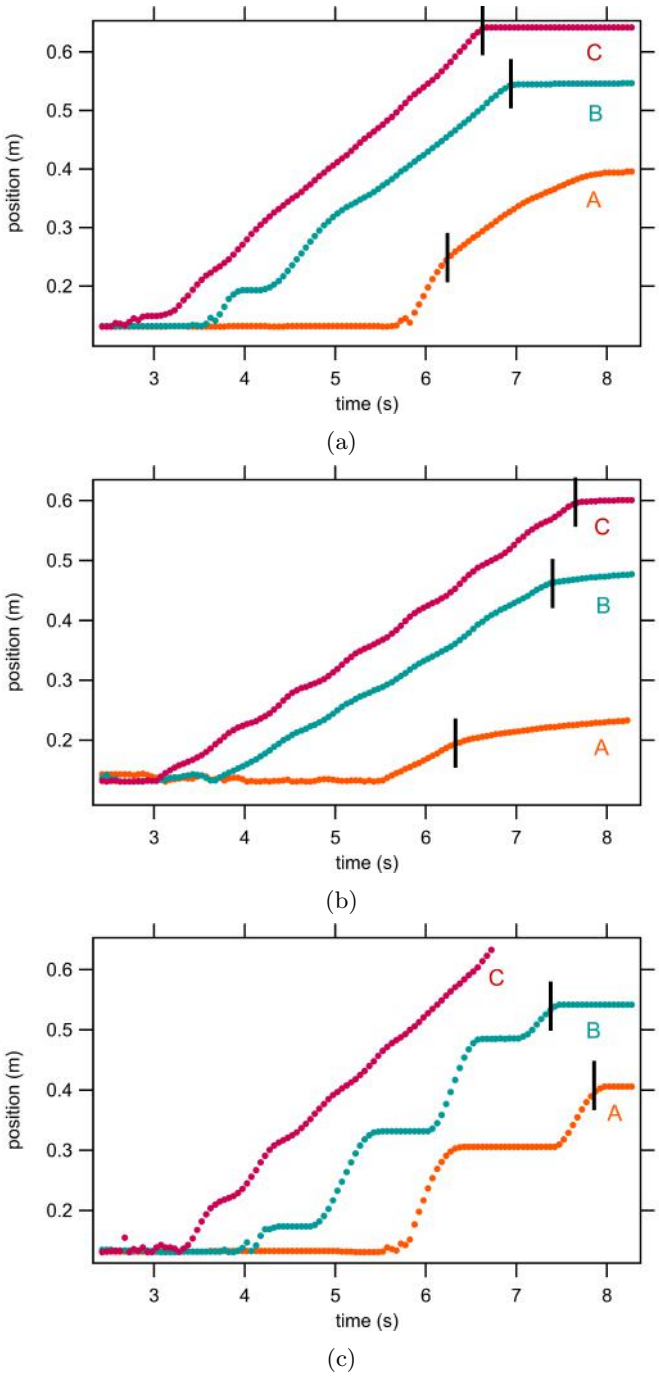

FIG. 7: Plots of position and time for a single block with three different sliding surfaces and three different springs, pulled by the same velocity driver. Each block slides over a PVC mat with either (a) aluminum (Al), (b) nitrile, or (c) cardstock. Orange traces are of spring A, green are spring B, and red are spring C, where $k_C > k_B > k_A$. Vertical black bars indicate the point at which the driving cart comes to a stop.

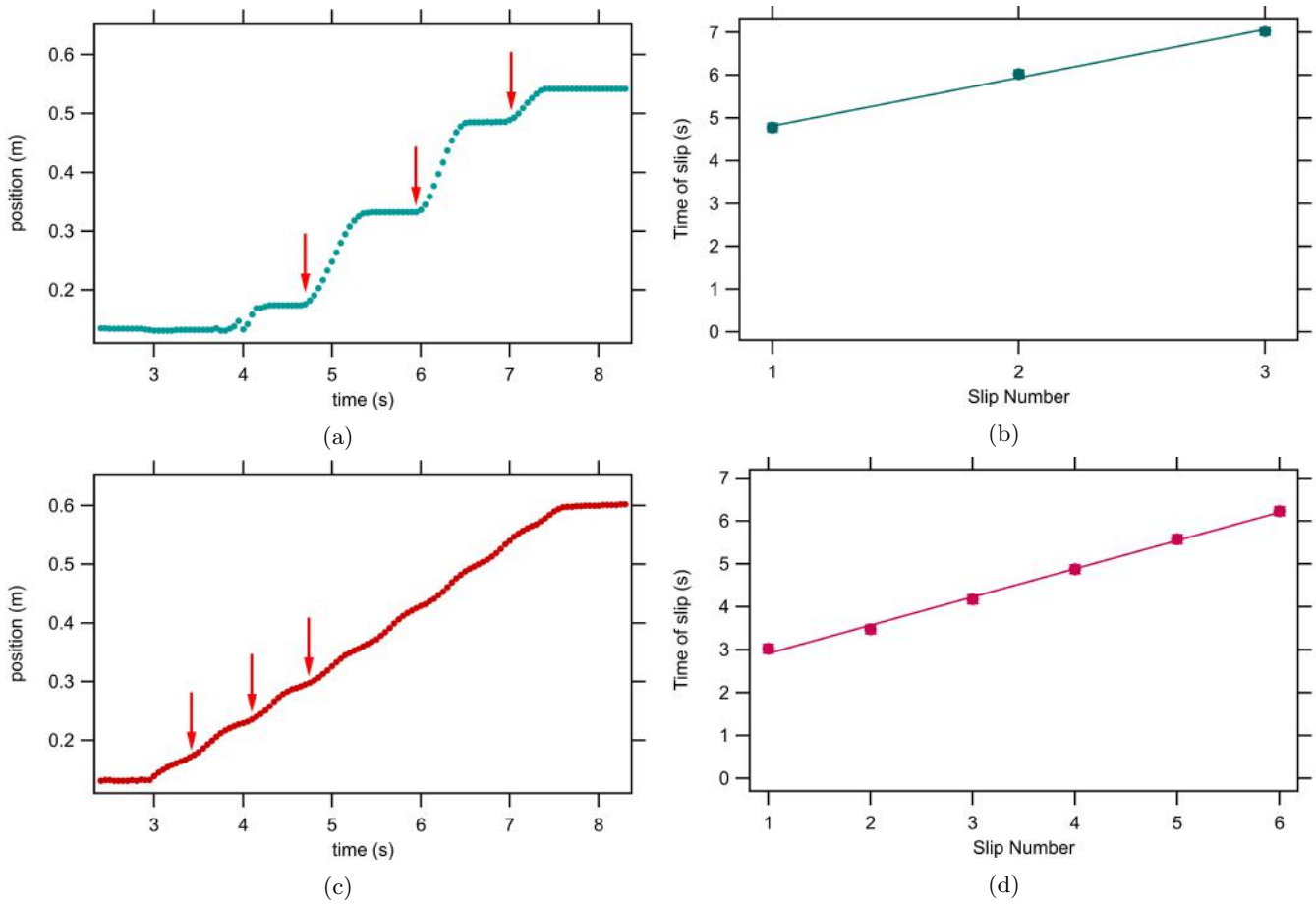

FIG. 8: Clear examples of the periodicity of slip events. Left: Position data demonstrating periodic slips, for (a) cardstock with spring B or (c) nitrile with spring C. The red arrows indicate the first few slip occurrences for each material. Right: The corresponding time-of-slip data for each position plot. The time of a given slip is given by the start of the slip, pointed to by the red arrows on the left plots. The linear fits to (b) and (d) indicate a periodic slip occurrence for each system.

for observations of true longterm behavior. However, if cardstock were velocity-strengthening the stick-slip motion would likely damp quickly to steady sliding, as seen for aluminum in Fig. 7a, and this is not the case. Thus, given the periodic stick-slick motion seen in Fig. 7c, cardstock most resembles a velocity-weakening system of the three materials used in combination with PVC. From this we can conclude that the cardstock-PVC contact is characterized by $(a - b) < 0$ and so the decrease of friction stress throughout a whole slip is larger than the stress increase at the onset of a slip.

One may wonder, if cardstock *is* velocity-weakening, then why does the trace for spring C damp to stable sliding? Recall that spring C corresponds to a higher critical stress σ_c than springs B and A, and so the curve in Fig. 4 is shifted to the right. Thus, for a high enough slip velocity, the system can transition from unstable to stable *without self-sustained oscillations* by increasing k so that the point falls beneath the stability curve sufficiently far left of the critical stress. This appears to be the case in Fig. 7c, where a driving voltage 2.6 V corresponds to a high enough slip velocity that the region of self-sustained oscillations is missed entirely as σ_c increases. Of course, the slip velocity is not necessarily constant for each trace of Plot 7c, particularly given that V_0 increases with increasing k. However, these variations in slip velocity V are likely negligible compared to the more substantial differences in spring strength, unless the system is quite close to the threshold curve of Fig. 4.

Possibly the easiest material to characterize is aluminum – a distinctly velocity-strengthening system. This property makes sense in consideration of the observable material properties of aluminum, such as the relative rigidity compared to the other materials, suggesting a higher a value. As one would expect for a velocity-strengthening system, stick-slip behavior can occur under certain conditions, but it is not *regular* stick-slip. Rather, any perturbations to the motion are quickly damped as the block settles to steady sliding, regardless of the spring strength.

The trickiest system to characterize is certainly nitrile. The data for spring A is limited due to the constrained available sliding distance, and the remaining two traces exhibit sustained oscillations. This might suggest that nitrile is velocity-weakening and the region of self-sustaining oscillations in Fig. 4 is large enough to contain the system even as the critical stress is shifted to the right; however, this would not explain why the oscillations become *more* pronounced for larger k. In fact, this behavior is counter-intuitive in the context of Fig. 4 which implies that increasing k would make the oscillations *less* pronounced. This behavior could be an anomaly, or it may be a result of special material properties of nitrile not considered in the theory presented in this paper. Alternatively, nitrile could be velocity-strengthening and the total sliding distance is not long enough to characterize the longterm behavior. Regardless, this data is inconclusive regarding the characterization of nitrile, other than that there may be a preference for small oscillations or "tremors" instead of stick-slip motion, and these tremors are periodic as seen in Fig. 8.

V. CONCLUSIONS

The position data for a one-block and spring model driven at a constant velocity was analyzed for three combinations of sliding materials, and three different springs. The metal-PVC system was determined to be velocity-strengthening as the block settled to stable sliding instead of stick-slip motion. The cardstock-PVC system was determined to likely be velocity weakening due to the appearance of regular stick-slip; however, further trials taken over a longer total sliding distance would need to be completed to better determine the longterm behavior of the system. The nitrile-PVC system yielded inconclusive results regarding whether the system was velocity-weakening or strengthening, but it did exhibit periodic tremors which may be self-sustaining.

The observed properties of these materials, in the context of a block-spring experiment, may be analogous to different kinds of rock properties that affect fault interactions during earthquakes, and this is something to be researched in future work. Furthermore, while this paper examines some of the types of simple earthquake oscillations that can be modeled experimentally, there are lots of complex and chaotic behaviors to explore in this system. The nonlinear dynamical behavior of earthquakes is one of the important areas of current research in geophysics. Developing experiments to probe 2, 3, and eventually any n-block arrays would be a logical progression to the experimentation done in this paper. A two-block model was even briefly explored in the course of this experiment, but the complexity of that system fell outside the scope of this paper.

Regarding the specific systems examined in this paper, further experimentation is needed to quantitatively characterize the materials. The constants a and b can be measured with more sophisticated techniques than used in this experiment, as well as the characteristic length D_c. Determination of these constants is an important next step in characterizing these materials as velocity-weakening or strengthening.

Furthermore, there are important improvements to be made to the experimental setup. The relatively short sliding surface created noticeable issues for the weaker spring A, as the cart would drive nearly the entire length of the platform before the block slipped. This could be improved by constructing a much longer sliding surface, at least two or three times the current length. Furthermore, future work would benefit from a higher geared motor that can generate more torque. This would allow for a much more stable driving velocity where the motor's function is not impeded by the resistance due to the block's friction.

VI. ACKNOWLEDGEMENTS

Special thanks to Tim Siegenthaler for help designing and constructing the block-spring apparatus, and aiding in modifications to the design throughout experimentation, as well as Dr. Lehman for guidance throughout the process of designing and executing this project, and to Katie Shideler and Andrew Kunkel for help with this experiment.

[1] R. Burridge, L. Knopoff. Model and theoretical seismicity. *Bulletin of the Seismological Society of America*, **57**(3), 1967.

[2] James H. Dieterich, Brian D. Kilgore. Direct observation of frictional contacts: New insights for state-dependent properties. *PAGEOPH*, **143**, 1994.

[3] Andy Ruina. Slip instability and state variable friction laws. *JOURNAL OF GEOPHYSICAL RESEARCH*, **88**(B12), 1983.

[4] Brittany A. Erickson, Björn Birnir, Daniel Lavallée. Periodicity, chaos and localization in a Burridge–Knopoff model of an earthquake with rate-and-state friction. *Geophysical Journal International*, **187**, 2011.

[5] Srdan Kostić, Igor Franović, Kristina Todorović, et al. Friction memory effect in complex dynamics of earthquake model. *Nonlinear Dynamics*, **73**, 2013.

[6] Cun Chen, Xueping Li, Jingli Ren. Complex dynamical behaviors in a spring-block model with periodic perturbation. *Complexity*, **2019**, 2019.

[7] Christopher H. Scholz. *The Mechanics of Earthquakes and Faulting.* Cambridge University Press, 3rd edition, 2019.